The 2010 IEEE/RSJ International Conference on
Intelligent Robots and Systems
October 18-22, 2010, Taipei, Taiwan

Input Shaping Control to Suppress Sloshing on Liquid Container Transfer Using Multi-Joint Robot Arm

Wisnu Aribowo, Takahito Yamashita, Kazuhiko Terashima, and Hideo Kitagawa

Abstract— **Transfer of container filled with liquid may generate sloshing, considered an undesirable effect in many systems. This research explores the use of input shaping technique to suppress sloshing on transfer of liquid container using multi-joint robot arm. By input shaping principle, acceleration command is shaped using two impulses in such a way to cancel each other's response. Position trajectory is then translated as joint angles trajectory, which is then fed to Mitsubishi PA10-7C robot arm. Simple pendulum model with damping element is applied to analyze sloshing phenomena. Experimental results show that the employed input shaping technique reduces sloshing during and after container transfer.**

I. Introduction

During transfer of container filled with liquid, oscillation of the free surface of the liquid, or sloshing, may occur. The sloshing occurs more on a high speed transfer, where high acceleration and deceleration is imposed on the system. This is undesirable on some system, for example in molten metal transfer of casting process where too much sloshing may cause spill-over, reduce temperature, and induce contamination of molten metal being transferred. Therefore, sloshing should be suppressed while maintaining high container transfer speed for productivity reason.

Various approaches have been used by researchers to tackle sloshing suppression problem. Feedback control of closed loop approach uses sensor measurements as feedback to generate input in a closed loop. Solutions using this approach present good and relatively robust control ability toward disturbances. Examples include generalized PI control [2] and sliding mode controller [3].

On the other hand, feedforward approach [6-9] does not require sensor measurement feedback, yet can provide good performance assuming that natural frequency and damping factor of the system are known beforehand. Author's group, Terashima *et al*. [7], developed Hybrid Shape Approach (HSA) using a notch-filter and obtained good results for sloshing suppression control. This approach is very practical, because the detailed model of sloshing is not required, except for natural frequency of liquid and transfer model of container. The result on sloshing suppression and positioning of container is very nice with good robustness, because HSA considers both characteristics such as time-domain in container transfer and frequency domain in sloshing suppression. However, if the sloshing phenomenon is mathematically modeled, faster transfer control with sloshing suppression can be expected based on the process model. If sloshing phenomena can be modeled by a series of second order transfer function comprised of mass, spring, and damper, input shaping approach developed by Singer and Seering [1] is one of most practical control approach. In input shaping approach, residual vibration is completely suppressed for the vibration systems including higher model oscillation, and the fastest control input in case of using only the same sign of control input can be obtained.

This approach is found useful in suppressing vibration of many kinds of flexible structures, for example robot arm and overhead crane, as well as sloshing suppression. In a molten metal transfer of casting process, it is difficult to do accurate sensing of liquid level in a real time manner. In this case, the use of input shaping technique is particularly useful.

Automated method of molten metal transfer typically involves specially-built large structure that takes space and lacks flexibility in positioning and orienting container. The use of robot arm having many degrees-of-freedom for this

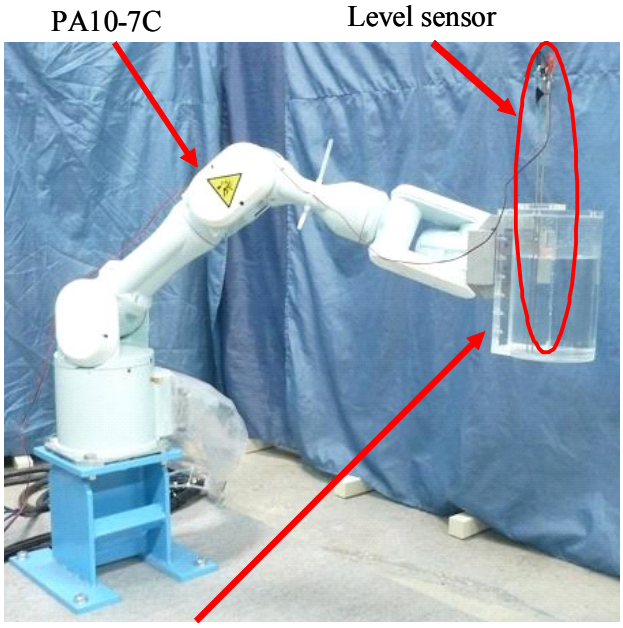

Fig. 1. Complete setup of the liquid transfer system.

Wisnu Aribowo, Takahito Yamashita, and Kazuhiko Terashima are with Department of Mechanical Engineering, Toyohashi University of Technology, Aichi 441-8580, Japan (e-mail: {wisnu, t-yamashita, terasima}@syscon.me.tut.ac.jp).

Hideo Kitagawa is with Department of Electronic Control Engineering, Gifu National College of Technology, Japan (e-mail: hkita@gifu-nct.ac.jp).

purpose, as proposed by this research, is novel. Advantages include relatively small footprint, improved speed and flexibility. However, they come with increased difficulty in control. Automatic parameter identification software is also developed in this research. Integration of automatic parameter identification method and input shaping approach is valuable, and will be a good basis for our future research on sloshing suppression.

This research explores the use of input shaping technique to suppress sloshing on transfer of liquid container using multiple degree-of-freedom robot arm. Section II presents the liquid transfer system construction. Section III explains in detail modeling of the system, while simulation and experiment result are presented and discussed in Section IV.

II. System Construction

The liquid transfer system concerned uses 7 degree-of-freedom Mitsubishi PA10-7C robot arm. Weighing only 40 kilograms, its longest arm reach is 1 meter, and can carry up to 10 kilograms of load on its arm tip. A cylindrical container, 150 mm in diameter and 250 mm in height, is mounted on the robot arm tip. Electric-resistance level sensor is attached to the container, placed on one side of the cylinder to measure height of liquid over time. It works by detecting changes in the resistance between two electrodes. Height fluctuation detected represents magnitude of sloshing. Figure 1 shows picture of the robot arm holding the container with level sensor attached. Liquid container is shown in Figure 2.

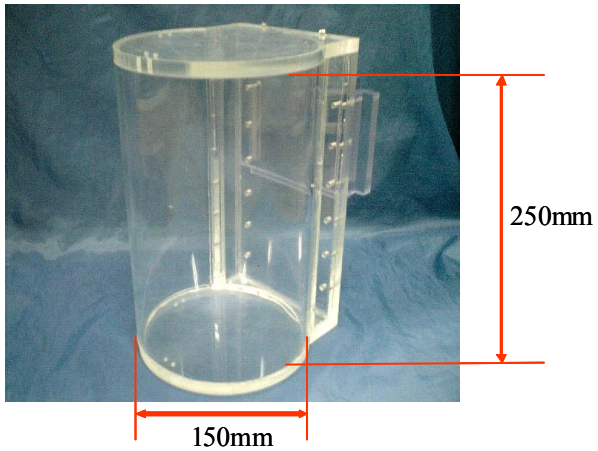

Fig. 2. Liquid container.

III. Modeling and Control Design

A. Robot Arm

Axis placement of the robot arm is shown in Figure 3. One of the arm joints, the S3 joint, is locked so that practically only six joints are actively used because redundancy of arms is not necessary for the present purpose in this paper, but required in next step to avoid obstacles. The active joints are S1, S2, E1, E2, W1, and W2. Thus six axes are assigned, one on each active joint. Figure 4 shows robot arm link dimension.

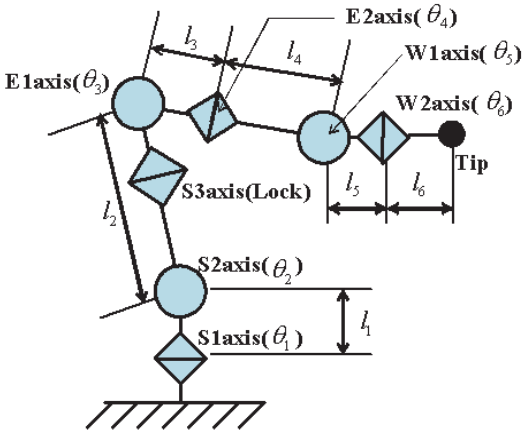

Fig. 3. Axis placement of robot arm.

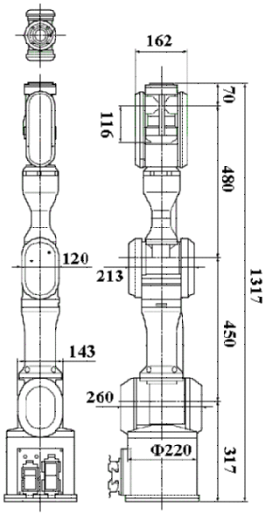

Fig. 4. Robot link dimension.

Inverse kinematics is used to translate tip position to each joint angle. Rotation matrix and translation matrix for each axis *i* is defined by:

$$
\left.\begin{aligned}
R_{xi} &= \begin{bmatrix} 1 & 0 & 0 \\ 0 & \cos\theta_i & -\sin\theta_i \\ 0 & \sin\theta_i & \cos\theta_i \end{bmatrix} \\
R_{yi} &= \begin{bmatrix} \cos\theta_i & 0 & \sin\theta_i \\ 0 & 1 & 0 \\ -\sin\theta_i & 0 & \cos\theta_i \end{bmatrix} \\
R_{zi} &= \begin{bmatrix} \cos\theta_i & -\sin\theta_i & 0 \\ \sin\theta_i & \cos\theta_i & 0 \\ 0 & 0 & 1 \end{bmatrix} \\
L_{xi} &= \begin{bmatrix} l_i & 0 & 0 \end{bmatrix}^T \\
L_{yi} &= \begin{bmatrix} 0 & l_i & 0 \end{bmatrix}^T \\
L_{zi} &= \begin{bmatrix} 0 & 0 & l_i \end{bmatrix}^T
\end{aligned}\right\} \quad (1)
$$

Relation between position (x, y, z) and orientation (φ, θ, ψ) of the arm tip and joint angles is as follows:

$$\begin{aligned}\begin{bmatrix} x & y & z \end{bmatrix}^T = R_{z1}(L_{z1} + R_{y2}(L_{z2} + R_{y3}(L_{z3} \\ + R_{z4}(L_{z4} + R_{y5}(L_{z5} + R_{z6}L_{z6})))))\end{aligned} \quad (2)$$

$$\left.\begin{aligned}\phi &= \tan^{-1}\left(\frac{T_{23}}{T_{13}}\right) \\ \theta &= \cos^{-1}\left(T_{33}\right) \\ \psi &= \tan^{-1}\left(\frac{T_{32}}{T_{31}}\right)\end{aligned}\right\} \quad (3)$$

, where matrix $\boldsymbol{T}$ is product of all rotation matrices:

$$\begin{bmatrix} T_{11} & T_{12} & T_{13} \\ T_{21} & T_{22} & T_{23} \\ T_{31} & T_{32} & T_{33} \end{bmatrix} = R_{z1}R_{y2}R_{y3}R_{z4}R_{y5}R_{z6} \quad (4)$$

We use vector $\boldsymbol{P}$ to denote position and orientation of robot arm tip and $\boldsymbol{\theta}$ for joint angles:

$$P = \begin{bmatrix} x & y & z & \phi & \theta & \psi \end{bmatrix}$$

$$\theta = \begin{bmatrix} \theta_1 & \theta_2 & \theta_3 & \theta_4 & \theta_5 & \theta_6 \end{bmatrix}^{\cdot}$$

Values of joint angles decide position and orientation of the robot arm tip. Relation between $\boldsymbol{P}$ and $\boldsymbol{\theta}$ is as follows:

$$P(t) = f\left\{\theta(t)\right\} \quad (5)$$

$$\dot{P}(t) = J\left\{\theta(t)\right\}\dot{\theta}(t) \quad (6)$$

, where $\boldsymbol{J}$ is the 6×6 Jacobian matrix. Thus derivative of $\boldsymbol{\theta}$ can be calculated from derivative of $\boldsymbol{P}$, provided that $\boldsymbol{J}$ is invertible:

$$\dot{\theta}(t) = J^{-1}\left\{\theta(t)\right\}\dot{P}(t) \quad (7)$$

Using this procedure, joint angles trajectory can be constructed from arm tip position trajectory.

B. Sloshing Model

Sloshing inside open container can be well represented by equivalent mechanical models, either a pendulum model or spring-mass model. One approach is by using simple pendulum model [4,6], where one pendulum represents one sloshing mode. Damper is added to the pendulum model to represent viscosity and friction of liquid with container walls. Considering only fundamental sloshing mode, which is dominant in container transfer sloshing, and neglecting other subsequent minor modes, the pendulum model as shown in Figure 5 can adequately represent the dynamics of sloshing in lateral direction.

In this model, planar liquid surface is perpendicular to the pendulum, which swings as container accelerates (or decelerates) by α, forming angle θ between planar liquid surface and horizontal line. Coefficient c represents damping effect of liquid viscosity and friction of liquid with container wall.

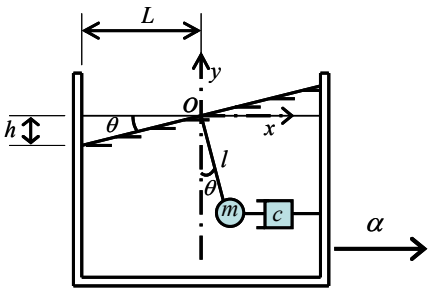

Fig. 5. Pendulum model of one-mode sloshing.

By considering moment balance around fulcrum of the pendulum, dynamics of the model can be described by the following equation:

$$\begin{aligned}J\frac{d^2\theta}{dt^2} = -c\frac{d(l\theta)}{dt}l\cdot\cos^2\theta - mgl\cdot\sin\theta \\ + m\alpha l\cdot\cos\theta\end{aligned} \quad (8)$$

, where J ($= ml^2$) is moment of inertia. The liquid level h on the side wall equals $L\cdot\tan(\theta)$. Considering only small value of θ, linear approximation of the above non-linear model is as follows:

$$\ddot{\theta} = -\frac{c}{m}\dot{\theta} - \frac{g}{l}\theta + \frac{\alpha}{l} \quad (9)$$

$$h = L\alpha \quad (10)$$

Transfer function between liquid level h and lateral acceleration α is thus described by the following equation:

$$\frac{h(s)}{\alpha(s)} = \frac{L/l}{s^2 + \frac{c}{m}s + \frac{g}{l}} \quad (11)$$

Comparing above equation to second-order damped linear oscillator with natural frequency ω_n and damping ratio ζ gives:

$$\omega_n = \sqrt{\frac{g}{l}} \quad (12)$$

$$\zeta = \frac{c}{2m}\sqrt{\frac{l}{g}} \quad (13)$$

, where m is mass of liquid, and equivalent pendulum length l (m) and coefficient of viscosity c (Ns/m) are identified by agreement of simulation and experiments as shown in next chapter.

C. Input Shaping Control

An uncoupled, linear, vibratory system of any order can be specified as a cascaded set of second-order poles with the decaying sinusoidal response:

$$\begin{aligned}y(t) = \left[A\frac{\omega_0}{\sqrt{1-\zeta^2}}\exp\left(-\zeta\omega_0(t-t_0)\right)\right] \\ \cdot\sin\left(\omega_0\sqrt{1-\zeta^2}\left(t-t_0\right)\right)\end{aligned} \quad (14)$$

, where A is amplitude of the impulse, ω_0 is the undamped natural frequency of the plant, ζ is the damping ratio of the plant, t is time, and t_0 is time of the impulse input [1].

For a system with only one mode of vibration, given impulse of amplitude 1 at time (t_0) = 0, the response will be:

$$y_1(t) = \left[\frac{\omega_0}{\sqrt{1-\zeta^2}} \exp\left(-\zeta\omega_0 t\right) \right] \sin\left(\omega_0\sqrt{1-\zeta^2}\,t\right) \qquad (15)$$

In order to suppress vibration by the above first impulse, we add second impulse at time ΔT such that response of the two impulses cancel out each other, as shown in Figure 6. Response of the second impulse is thus as follows:

$$y_2(t) = \left[K \frac{\omega_0}{\sqrt{1-\zeta^2}} \exp\left(-\zeta\omega_0 (t-\Delta T)\right) \right] \cdot \sin\left(\omega_0\sqrt{1-\zeta^2}\,(t-\Delta T)\right) \qquad (16)$$

, where K is the amplitude of second impulse.

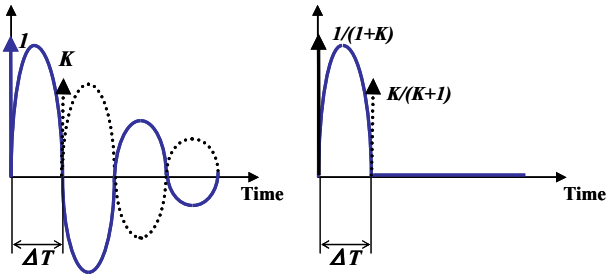

Fig. 6. Principle of input shaping

By setting sum of $y_1(t)$ and $y_2(t)$ to 0 for all time after ΔT, we obtain the magnitude (K) and time (ΔT) of second impulse as follows:

$$K = \exp\left(-\frac{\zeta\pi}{\sqrt{1-\zeta^2}} \right) \qquad (17)$$

$$\Delta T = \frac{\pi}{\omega_0\sqrt{1-\zeta^2}} \qquad (18)$$

Adjustment should be made so that the sum of the two impulses equals 1 (thus the command does not go beyond maximum value), giving $1/(1+K)$ as first impulse magnitude and $K/(1+K)$ as the second impulse magnitude.

The above formula for single mode can be generalized to higher modes, i.e. $N \geq 2$, as explained in Duong *et al.* [10]. Impulse sequences built independently for each system mode convolve with each other to form an impulse sequence that reduces multi-mode system vibration. Just as in the single-mode case, the impulse sequence in higher modes is normalized and convolved with commanded input to make vibration-suppressed input to the system.

To generate preshaped input for multimode vibration, the magnitude and time of the second impulse for each mode are calculated the same as in (17) and (18):

$$K_i = \exp\left(-\frac{\zeta_i\pi}{\sqrt{1-\zeta_i^2}} \right) \qquad (19)$$

$$\Delta T_i = \frac{\pi}{\omega_{0i}\sqrt{1-\zeta_i^2}} \quad , (i = 1, 2, ..., N) \cdot \qquad (20)$$

Assuming that commanded input is $u(t)$, preshaped input $u_p(t)$ for multi-mode system vibration is calculated in three steps:

- *Step 1*: Calculate preshaped input $u_1(t)$ corresponding to mode 1 from commanded input $u(t)$:

$$u_1(t) = \frac{1}{K_1+1}u(t) + \frac{K_1}{K_1+1}u(t-\Delta T_1) \qquad (21)$$

- *Step 2*: Calculate preshaped input $u_i(t)$, where $i \geq 2$ corresponding to mode i from preshaped input $u_{i-1}(t)$ of previous mode (i-1):

$$u_i(t) = \frac{1}{K_i+1}u_{i-1}(t) + \frac{K_i}{K_i+1}u_{i-1}(t-\Delta T_i) \qquad (22)$$

- *Step 3*: Preshaped system input $u_p(t)$ is preshaped input $u_N(t)$ corresponding to mode N calculated from preshaped input $u_{N-1}(t)$ of previous mode (N-1): $u_p(t) = u_N(t)$.

D. Identification Method of Parameters

There are two parameters of the sloshing system that need to be identified for implementation of input shaping: natural frequency ω_0 and damping ratio ζ. We develop automatic parameter identification method for that purpose. First, power spectrum of the sloshing is obtained by Fast Fourier Transform (FFT) method, in which natural frequencies of the sloshing system are identified as the frequencies of spectrum peaks. The number of peaks corresponds to the number of sloshing modes in the system. Each separated mode is then transformed back to time domain in order to identify damping ratio. Damping ratio ζ_i determines how much the sloshing amplitude decreases every cycle, by an amount of $e^{-\zeta_i\omega_i t}$ according to the vibration model shown in Equation (14). Thus, by identifying the maximum sloshing amplitude in each cycle and applying fitting to those values, damping ratio of the system can be identified. Details are explained in reference [11], and omitted due to limitation of paper page.

IV. Simulation and Experiment

In this paper, only straight path transfer is focused from start point to end point. Liquid transfer on curved path induces nonlinear phenomena such as centrifugal force, and it is difficult to exactly suppress sloshing in curve transfer by only input shaping method. Therefore, curve transfer with sloshing suppression using robot arm is not considered in this experiment, but will be reported in near future.

For this experiment, robot arm has to move the container on a straight path from start point (700, -500, 250) to end point (700, 500, 250). Height and mass of liquid inside container is

170 mm and 3 kg, respectively. Maximum acceleration and velocity is 2 m/s^2 and 0.5 m/s, respectively.

Natural frequency for fundamental mode of sloshing of this particular setting is 15.506 rad/s = 2.469 Hz. From this value and (12), we obtain equivalent pendulum length (l) of 0.0408 meter. Value of damping ratio ζ was estimated, and coefficient of viscosity c can be calculated from (13), found to be equal 1.02 Ns/m. Table I lists all parameter values of our system.

TABLE I
PARAMETER VALUES

Parameter	Value	Unit
Equivalent pendulum length, l	0.0408	m
Coefficient of viscosity, c	1.02	Ns/m
Mass of liquid, m	3	kg
Nominal level, h_s	0.17	m
Radius, L	0.075	m
Gravity acceleration, g	9.8	m/s^2

By using those parameter values, input shaper is constructed, with K equals 0.966 and time between two impulses (ΔT) equals 0.21 second. Figure 7 shows the shaped acceleration profile as compared to the unshaped one. The shaped acceleration profile takes slightly longer time because of the input shaping delay.

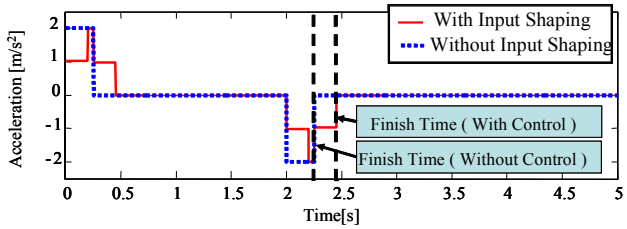

Fig. 7. Acceleration and deceleration profile

Container position trajectory, shown in Figure 8(a), is then generated from the acceleration profile. Inverse kinematics procedure translates the position trajectory to robot joint angles trajectory as shown in Figure 8(b). Those joint angles are then used as command to move the robot arm.

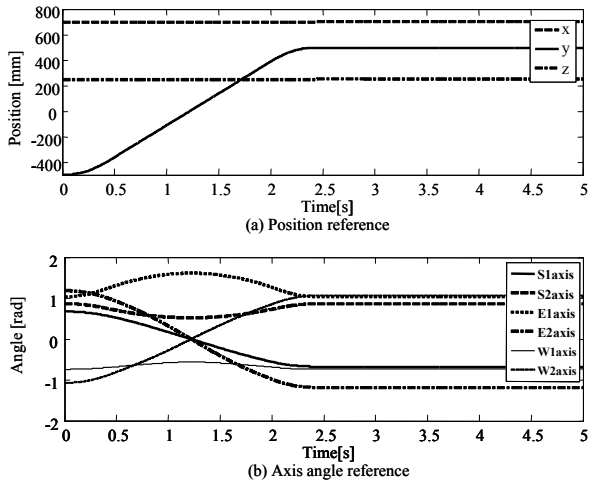

Fig. 8. Shaped position reference and joint angle reference

Using the joint angle reference, simulation is conducted. The result is shown in Figure 9. Without shaping, liquid surface oscillates relatively highly. Small damping of the liquid causes the sloshing stays during transfer and even long after transfer. Effect of shaping is apparent, in that water level displacement occurs only when container accelerates and decelerates, quite effectively suppressing sloshing of the liquid transfer system considered.

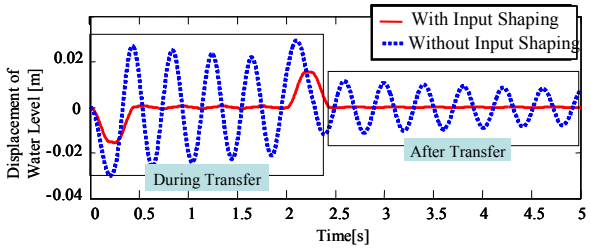

Fig. 9. Simulation result

Experiment is conducted by supplying axis angle reference to the PA10 robot motion controller. Figure 10 shows the experiment result, showing quite high confirmation with the simulation result regarding the shape, amplitude, and period of vibration. This shows that the pendulum model is representative for our sloshing case. It is easily seen that sloshing is much lower when input shaping is performed, both during and after transfer. However, it should be noted that transfer time required by input shaping approach (2.46 second) is slightly longer than that without input shaping (2.25 second).

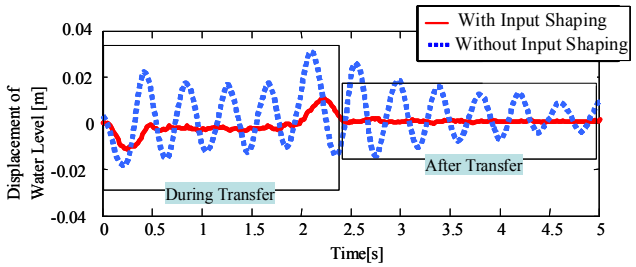

Fig. 10. Experimental result

In practice, liquid container transfer usually involves several movements performed one after another. We have carried out another experiment to show the performance of input shaping for that kind of scenario. Figure 11 shows the robot movement path, which consists of four straight segment paths, parallel to either X or Y axis. Level sensors are suitably placed to capture highest displacement of liquid level. Each path has different acceleration rate, but same acceleration time (0.25 second for unshaped case). Deceleration rate for each segment is the same as its acceleration rate. Waiting times are added between segment paths to give enough time for residual liquid vibration to die out. Table II lists acceleration rate, maximum velocity, and movement start time of each path.

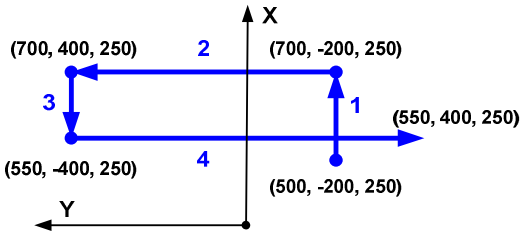

Fig. 11. Robot movement path of second experiment

TABLE II
DATA FOR SECOND EXPERIMENT

Segment path	Acceleration [m/s^2]	Max. vel. [m/s]	Movement start time [s]
1	0.8	0.2	0
2	2	0.5	10
3	0.6	0.15	20
4	1.6	0.4	30

As before, robot arm tip position trajectory is generated from acceleration profile, for both shaped and unshaped cases. Robot joint angles reference could then be obtained using inverse kinematics. Figure 12 shows acceleration profile, joint angles reference, and water level displacement from the experiment. The water level displacement shown in the graph is combination of obtained values from two sensors: path 1 and 3 from 'X' sensor, path 2 and 4 from 'Y' sensor. The purpose is to show highest water level displacement on each segment path.

Container movements without shaping generate much sloshing, as expected. Sloshing tends to be larger on movements with high acceleration. Highest sloshing occurs on path 2, while lowest sloshing occurs on path 3. The experimental result also shows that the employed input shaping technique succeeds in suppressing sloshing in all segment paths, and it is most effective when acceleration is high. This raises confirmation on the usefulness of input shaping technique in sloshing suppression of high speed transfer of liquid container.

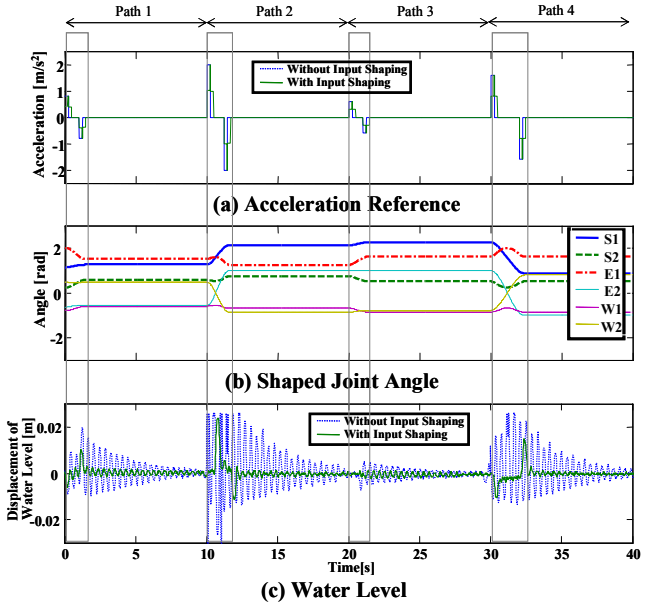

Fig. 12. Result of second experiment: (a) acceleration reference profile, (b) shaped joint angles (c) displacement of water level

V. CONCLUSION

In this paper, sloshing suppression by input shaping principle on liquid transfer using robot arm has been achieved. This initial work on sloshing control for this kind of system looks promising, as already shown in this paper. The developed automatic parameter identification method will be a good basis for our future researches. Future work is directed to address robustness issue, as well as transfer on curved path to exploit the flexibility, such as obstacle avoidance, offered by many-degrees-of-freedom robot arm with redundancy.

REFERENCES

[1] N. C. Singer and W. P. Seering, "Preshaping command inputs to reduce system vibration", *Journal of Dynamic System, Measurement, and Control*, vol. 112, pp. 76-82, 1990.

[2] H. Sira-Ramirez and M. Fliess, "A flatness based generalized PI control approach to liquid sloshing regulation in a moving container", in *Proceedings of the American Control Conference*, Anchorage, USA, 2002, pp. 2909-2914.

[3] B. Bandyopadhyay, P. S. Gandhi, and S. Kurode, "Sliding mode observer based sliding mode controller for slosh-free motion through PID scheme", *IEEE Transactions on Industrial Electronics*, vol. 56-9, pp. 3432-3442, 2009.

[4] J. T. Feddema , C. R. Dohrmann, G. G. Parker, R. D. Robinett, V. J. Romero, and D. J. Schmitt, "Control for Slosh-Free Motion of an Open Container", *IEEE Control Systems Magazine*, vol. 17-1, pp. 29–36, 1997.

[5] F. T. Dodge, "The New Dynamic Behavior of Liquids in Moving Container", Southwest Research Institute, San Antonio, Texas, 2000.

[6] K. Yano and K. Terashima, "Robust Liquid Container Transfer Control for Complete Sloshing Suppression", *IEEE Transactions on Control Systems Technology*, vol. 9-3, pp. 483-493, 2001.

[7] K. Terashima, K. Yano, K. Okamura, H. Kawagishi, and M. Watanabe, "An optimum design with sloshing suppression on container transfer control of molten metal using fluid dynamics model", *International Journal of Cast Metals*, vol. 15-4, pp. 435-440, 2002.

[8] K. Yano and K. Terashima, "Sloshing suppression control of liquid transfer systems considering 3D transfer path", *IEEE/ASME Transaction on Mechatronics*, vol. 10-1, pp. 8-16, 2005.

[9] Y. Shen, K. Terashima, and K. Yano, "Optimal control of rotary crane using straight transfer transformation method to eliminate residual vibration, *Transaction of the Society of Instrument and Control Engineers*, vol. 39-8, pp. 817-826, 2003.

[10] M. D. Duong, K. Terashima, T. Kamigaki, and H. Kawamura, "Development of a vibration suppression GUI tool based on input preshaping and its application to semiconductor wafer transfer robot", *International Journal of Automation Technology*, vol. 2-6, pp. 479-485, 2008.

[11] K. Terashima, Y. Masui, H. Kawamura, et al., "Vibration Characteristics Identification Device, Method and Transfer System", Japan Patent 2009-290143, December 22, 2009.